Journal of Power Sources 195 (2010) 8000–8005

Contents lists available at ScienceDirect

Journal of Power Sources

journal homepage: www.elsevier.com/locate/jpowsour

Membrane degradation mitigation using zirconia as a hydrogen peroxide decomposition catalyst

Shaohua Xiao[a,b], Huamin Zhang[a,*], Cheng Bi[a,b], Yining Zhang[a], Yuanwei Ma[a,b], Xianfeng Li[a], Hexiang Zhong[a], Yu Zhang[c]

[a] Lab of PEMFC Key Materials and Technologies, Dalian Institute of Chemical Physics, Chinese Academy of Sciences, Dalian 116023, China
[b] Graduate University of the Chinese Academy of Sciences, Beijing 100039, China
[c] Rongke Power Corporation, Limited, Dalian 116021, China

ARTICLE INFO

Article history:
Received 4 May 2010
Received in revised form 14 June 2010
Accepted 15 June 2010
Available online 23 June 2010

Keywords:
Degradation mitigation
Hydrogen peroxide decomposition
Zirconia
Durability
Rotating ring-disk electrode

ABSTRACT

Zirconia as a hydrogen peroxide decomposition catalyst is firstly investigated to mitigate the membrane degradation in terms of the in situ open circuit voltage (OCV) test and the ex situ Fenton test. OCV decay rate and fluorine emission rate (FER) are used to quantify the membrane degradation rate. The rotating ring-disk electrode (RRDE) is also employed to further confirm the effect. The ZrO_2-Nafion membrane exhibits more stable OCV and lower FER than the recast Nafion, suggesting that ZrO_2 nanoparticles have the potential to enhance membrane durability.

1. Introduction

There is a trade-off between power generation and environment around the world. Fuel cells are attractive alternatives to combustion engines for the electrical power generation due to their low emissions and high conversion efficiency [1]. Proton exchange membrane fuel cells (PEMFCs) are generally considered to be the most promising mobile applications [2]. Good durability is one of the most necessary characteristics for PEMFCs to be accepted as a viable product. The lifetime requirements vary significantly from different applications, e.g. 5000 h for car, up to 20,000 h for bus and up to 40,000 h for stationary applications [3]. The lifetime of PEMFCs is mainly determined by the chemical stability of the membrane [4], and H_2O_2 has usually been considered to be the species indirectly responsible for the membrane degradation [5,6].

Hydrogen peroxide can be generated either through the incomplete reduction of oxygen at cathode or the chemical combination of crossover gas and gas on the catalyst [6], and has been confirmed using a microelectrode [7]. Once generated, hydrogen peroxide can readily react with the trace transition metals in the membrane electrode assembly (MEA) [8] to generate free-radicals, which are capable of initiating the membrane degradation [9].

Normally two major approaches can be taken to minimize the membrane degradation: (1) the incorporation of a free-radical scavenger to get rid of free-radicals; (2) the impregnation of a hydrogen peroxide decomposition catalyst (HPDC) to lower the concentration of H_2O_2. For the former approach, cerium oxide was used as a regenerative free-radical scavenger due to the faster reversible redox reaction ($Ce^{3+} \leftrightarrow Ce^{4+} + e^-$) [10–12]. For the latter one, HPDCs such as MnO_2 and TiO_2 were introduced to the catalyst to enhance the membrane durability, but the hybrid catalyst activity is lower due to the harsh treatment with a strong acid [13,14]. Still some other catalysts like alkoxide of transition element or rare-earth element (Mn, Ti, Zr, etc.) have the ability to decompose the peroxide through hydrolyzation as well [15,16]. However, their effect on membrane degradation was just briefly proposed.

Zirconia as an inorganic additive is widely used to improve the membrane properties at high temperature/low humidity [17–23], and sulfated zirconia is usually employed as a super acid to enhance the membrane proton conductivity [24]. But the effect of zirconia in mitigating membrane degradation is still not clear.

In the present work, zirconia was prepared by the hydrothermal method and incorporated in the membrane as a hydrogen peroxide decomposition catalyst to enhance the membrane durability. The in situ open circuit voltage (OCV) test, the ex situ Fenton test and the rotating ring-disk electrode (RRDE) technique were employed to investigate the membrane degradation in detail. OCV decay rate

* Corresponding author. Tel.: +86 411 84379072; fax: +86 411 84665057.
E-mail address: zhanghm@dicp.ac.cn (H. Zhang).

0378-7753/$ – see front matter © 2010 Elsevier B.V. All rights reserved.
doi:10.1016/j.jpowsour.2010.06.052

and fluorine emission rate (FER) were used to quantify the membrane degradation rate.

2. Experimental

2.1. Catalyst preparation

Zirconia (ZrO_2) was prepared by the hydrothermal method [25]. 2.5 wt.% NH_3 solution was added dropwisely into 0.1 M $ZrO(NO_3)_2$ aqueous solution with vigorously stirring, and the final pH value of the slurry was about 10. The resulting white precipitate was aged at room temperature for 24 h with vigorous stirring, and then transferred into a stainless Teflon-lined 70 ml capacity autoclave. The autoclave was subjected to a hydrothermal treatment at 150 °C for 12 h. Then ZrO_2 nanoparticles were collected by centrifugation, washed with de-ionized water to remove ionic remnants, and dried at 60 °C under vacuum.

Pt-ZrO_2/C catalyst was prepared according to Liu et al. [26]. 300 mg Vulcan XC-72 (Carbot corp., BET: 235 $m^2\,g^{-1}$, denoted as C) was mixed with 60 ml isopropanol and stirred with a magnetic stirrer for 30 min. $ZrO(NO_3)_2$ was impregnated using a similar aqueous incipient wetness technique, dried at 90 °C, and calcined at 500 °C in N_2 for 3 h. The Pt-ZrO_2/C catalyst was prepared by the reduction of H_2PtCl_6 in an ethylene glycol (EG) solution on ZrO_2/C powders. The loading of Pt and ZrO_2 is 20 wt.% and 5 wt.%, respectively. For comparison, Pt/C catalyst with the same Pt loading was prepared in the same way.

2.2. Membrane preparation

The ZrO_2-Nafion membrane (denoted as ZrO_2-Nafion) was prepared by the solution-casting method. The solvent was evaporated to get Nafion® resin which was redissolved in DMF. The Nafion®/DMF solution and ZrO_2 nanoparticles were mixed ultrasonically to form the slurry. Then the slurry was poured onto a flat glass plate. The glass plate was first dried on a hot plate at 60 °C for 24 h then in a vacuum oven at 160 °C for 2 h. The loading of ZrO_2 nanoparticles in the membrane was kept at 3 wt.%. The thickness of the ZrO_2-Nafion was about 50 μm. The recast Nafion® membrane without ZrO_2 nanoparticles was prepared in a similar way. Re-acidification of the membranes was carried out by treating with 0.5 M H_2SO_4 solution for 1 h at 80 °C followed by the de-ionized water for 1 h at 80 °C.

2.3. XRD, SEM and TEM characterization

ZrO_2 nanoparticles was structurally characterized by XRD using a PW3040/60 X' Pert PRO (PANalytical) diffractometer equipped with a Cu Kα radiation source (λ = 0.15432 nm) in the 2θ range from 20° to 80° with angular step 10° min^{-1}.

SEM (JEOL 6360LV, Japan) was employed to observe the cross-section, which was made by freeze fracture from a strip of the composite membrane submerged in liquid nitrogen.

TEM image was recorded on a JEOL JEM-2000EX microscope operated at 120 kV. The ZrO_2 nanoparticles were ultrasonically suspended in the ethanol and a drop of the suspension was transferred to a copper grid and the ethanol was allowed to evaporate [27].

2.4. Membrane electrode assembly (MEA) fabrication and single cell test

The MEAs with 5 cm^2 active area were fabricated by a hot-pressing method at 140 °C and 1 MPa for 1 min. The Pt loadings and the dry Nafion loading are 0.3 mg cm^{-2} and 0.4 mg cm^{-2} in the anode, 0.7 mg cm^{-2} and 0.6 mg cm^{-2} in the cathode, respectively. The SGL carbon papers were employed in the gas diffusion layer (GDL). Two electrodes were hot-pressed onto a membrane to form a MEA. The MEA was placed in a single cell using the stainless steel as the end plates and the stainless steel mesh as the current collectors.

The single cells were run at a cell temperature of 80 °C, 0.2 MPa gas pressure and externally humidified H_2 and O_2 both at 80 °C, respectively. After the cell performance had been stable for 8 h, the cell voltages at different current densities were recorded.

2.5. Linear sweep voltammetry (LSV) measurement

The gas permeability of the membranes before and after OCV test was evaluated by measuring the limiting oxidation current densities of the permeating hydrogen using CHI 600B electrochemical workstation. H_2 gas (40 ml min^{-1}) was fed to the anode side of the cell while N_2 (100 ml min^{-1}) was fed to the cathode. By applying a dynamic potential to the cathode from 0 V to 0.6 V versus the anode with a scan rate of 5 mV s^{-1} at 0.2 MPa, 80 °C and 100% RH, the H_2 oxidation current was measured [28].

2.6. Membrane durability tests

The membrane durability was evaluated by both the ex situ Fenton's accelerated test and the in situ open circuit voltage (OCV) accelerated test. Membrane samples were respectively immersed in 40 ml Fenton solution (30 wt.% H_2O_2 solution and 20 ppm Fe^{2+}) at 80 °C for 3 h. A glass pipe was used to ensure that the membrane sample did not float into the head space of the vial. Gas pressure was released from the vessel through a little hole in the lid [29]. The 3 h durability test was repeated using a fresh Fenton solution. Membrane samples boiled for 30 h were taken out from the Fenton solution. All the replaced solution was collected for the further analysis.

The MEAs were subjected to the in situ OCV test at 80 °C, 0.2 MPa and 50% RH to assess the PEM degradation rate. H_2 gas was fed to the anode of the cell while O_2 was fed to the cathode. The gas flow rate was 40 ml min^{-1}. The test was run for 24 h for each MEA, and the drain water from the cathode and the anode was condensed in the cold-traps separately.

2.7. Fluorine emission rate (FER)

An ion chromatography system (ICS-90, DIONEX) was used to detect the concentration of the fluoride ions in the sample [30]. Prior to analysis, hydrogen peroxide must be completely decomposed to obtain the accurate and reproducible results [31].

2.8. Electrochemical measurement

The oxygen reduction reaction on the catalysts (Pt-ZrO_2/C, Pt/C) was analyzed by the rotating ring-disk electrode (RRDE) technique. The RRDE (VMP3 electrochemical station, Princeton Applied Research) consists of a glassy carbon disk and a platinum ring. The geometric surface areas of the ring/disk electrodes are 0.2475 and 0.1866 cm^2, respectively. A Nafion coating layer was deposited on the disk according to the following procedures: 5.0 mg sample, 1 ml ethanol and 50 μl Nafion solution (5 wt.%) were mixed ultrasonically to produce a catalyst ink; A 20 μl catalyst ink was spread on the disk surface and dried prior to use. A three-electrode electrochemical cell, which had a saturated calomel electrode (SCE) as the reference electrode and a platinum wire as the counter electrode, was employed. The electrolyte used was 0.5 M sulfuric acid. After the activation step, the ring potential was held at 1.0 V versus SCE, while the disk potential was varied from 1 V versus SCE to 0 V versus SCE at a sweep rate of 10 mV s^{-1} [13,32].

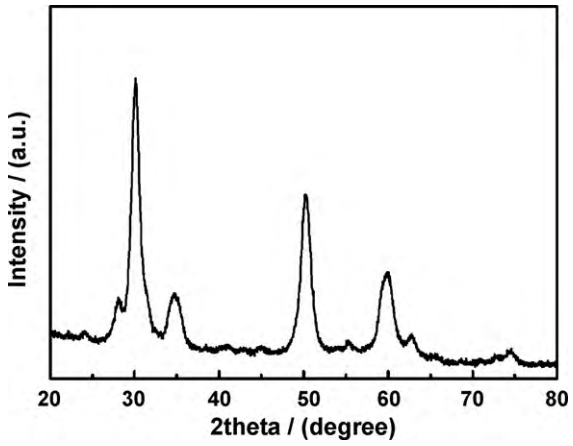

Fig. 1. XRD spectrum of ZrO_2 nanoparticles.

3. Results and discussions

3.1. Characterization of ZrO_2 nanoparticles

X-ray diffraction was employed to confirm the crystalline phase in ZrO_2 nanoparticles obtained by the hydrothermal method. Fig. 1 shows the XRD patterns of ZrO_2. The peaks at 2θ values of 30°, 34.5°, 50°, 60° are attributed to the tetragonal structure of ZrO_2 nanoparticles [33]. The average particle size of ZrO_2 nanoparticles is 5.8 nm, calculated by the Scherrer's formula [34]. The actual particle size of ZrO_2 nanoparticles, obtained by TEM (Fig. 2), is relatively larger than that value due to the unavoidable agglomeration. The size of ZrO_2 agglomerates is approximately 10 nm.

3.2. SEM image of membrane

To determine the cross-sectional morphology of ZrO_2-Nafion membrane, the SEM measurement was conducted and the result was shown in Fig. 3. It is observed that the cross-section of the membrane is dense and no obvious aggregation of ZrO_2 nanoparticles is found. This might be attributed to the nanometer-sized particles and good compatibility with Nafion® matrix [35].

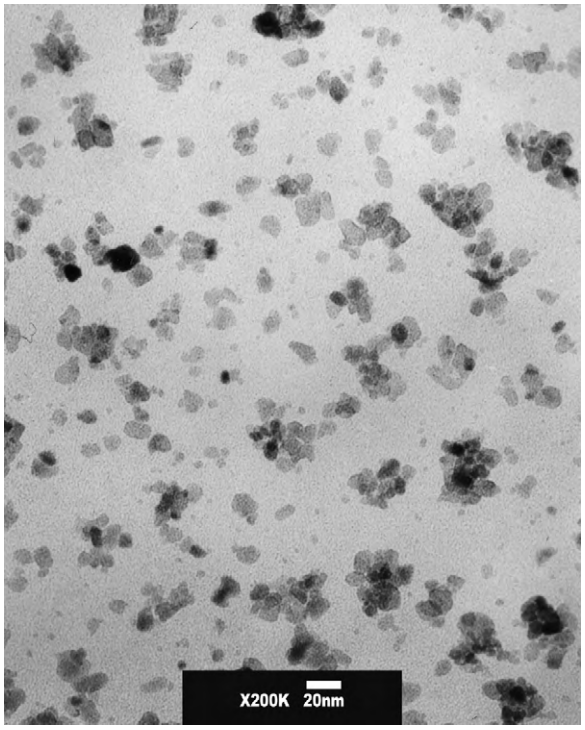

Fig. 2. TEM micrograph of ZrO_2 nanoparticles.

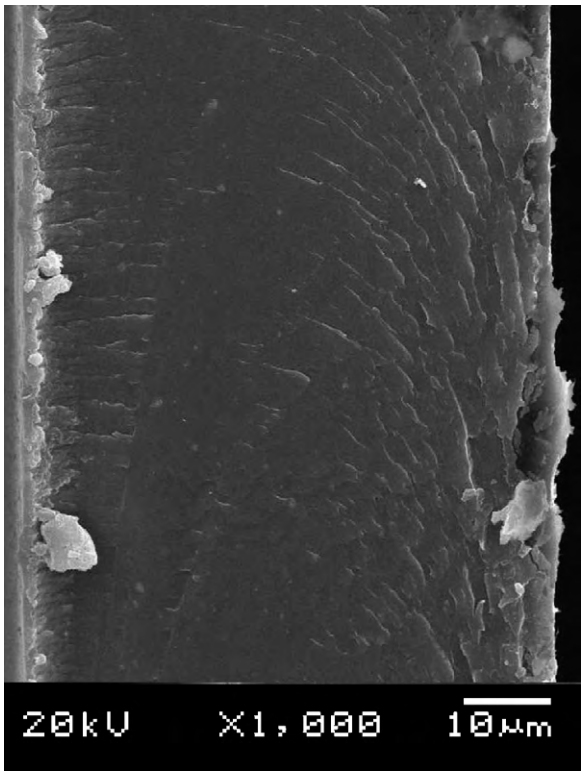

Fig. 3. SEM image of the cross-sectional morphology of ZrO_2-Nafion membrane.

3.3. Performance of PEMFCs operated under fully humidified conditions

Polarization curves are obtained under the fully humidified conditions at 80 °C and 0.2 MPa, with oxygen as the oxidant and hydrogen as the fuel (Fig. 4). It is observed that the cell performance with the ZrO_2-Nafion is slightly worse than that of the recast Nafion. The decrease in the cell performance with the ZrO_2-Nafion is ascribed to the increased proton-conductive resistance caused by incorporating non-proton-conductive ZrO_2 nanoparticles [36].

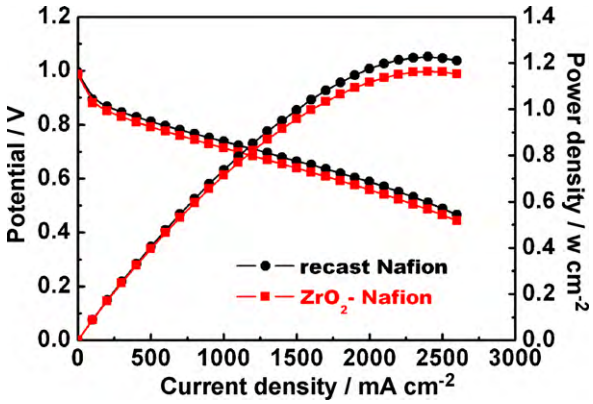

Fig. 4. Performance comparison of single cell employing different membranes (cell temperature: 80 °C; saturator temperature: 80 °C; RH: 100%; anode gas: H_2; cathode gas: O_2).

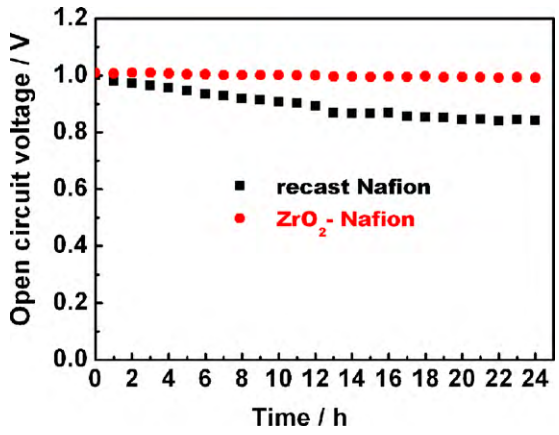

Fig. 5. Durability comparison of different membranes during OCV tests (cell temperature: 80 °C; saturator temperature: 64 °C; RH: 50%; anode gas: H_2; cathode gas: O_2; flow rate: 40 ml min^{-1} at anode and cathode; and duration: 24 h).

3.4. Membrane durability tests

3.4.1. In situ OCV accelerated test

In order to obtain a macroscopic estimate of the membrane degradation rate, OCV accelerated test was employed to evaluate the ZrO_2-Nafion and the recast Nafion based MEAs. As shown in Fig. 5, the ZrO_2-Nafion based MEA shows a more stable OCV than that of MEA with the recast Nafion. The OCV decay rates for the ZrO_2-Nafion and the recast Nafion are 0.8 mV h^{-1} and 6.6 mV h^{-1}, respectively. Meanwhile, the limiting current of the two MEAs is around 4 mA cm^{-2} before the OCV test (Fig. 6). After 24 h OCV accelerated test, the limiting current of the recast Nafion shows an increase while that of the ZrO_2-Nafion keeps constant. This suggests that the permeability of the recast Nafion increases after OCV test as well. To further confirm the conclusion, cross-sectional struc-

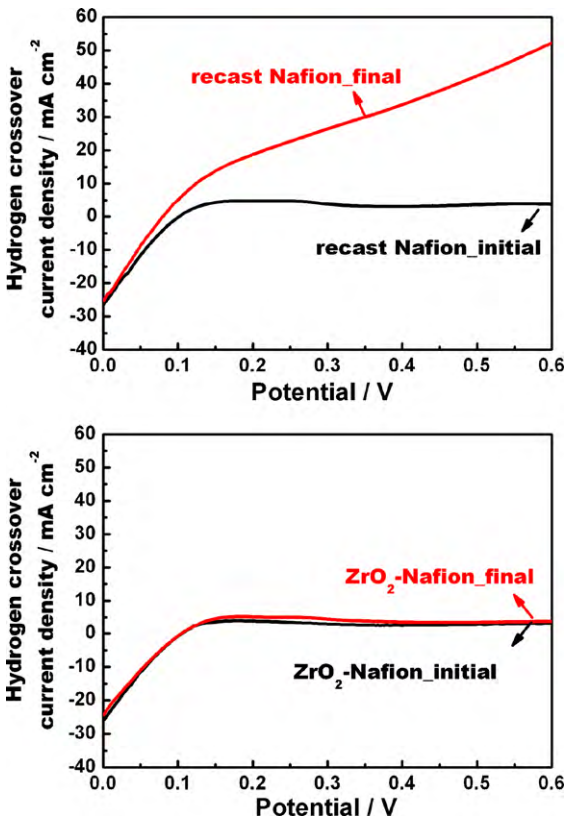

Fig. 6. Hydrogen crossover current density for H_2/N_2 cell with different membranes before and after OCV tests (cell temperature: 80 °C; saturator temperature: 80 °C; RH: 100%; anode gas: H_2; cathode gas: N_2; flow rate: 40 ml min^{-1} at anode and 100 ml min^{-1} at cathode).

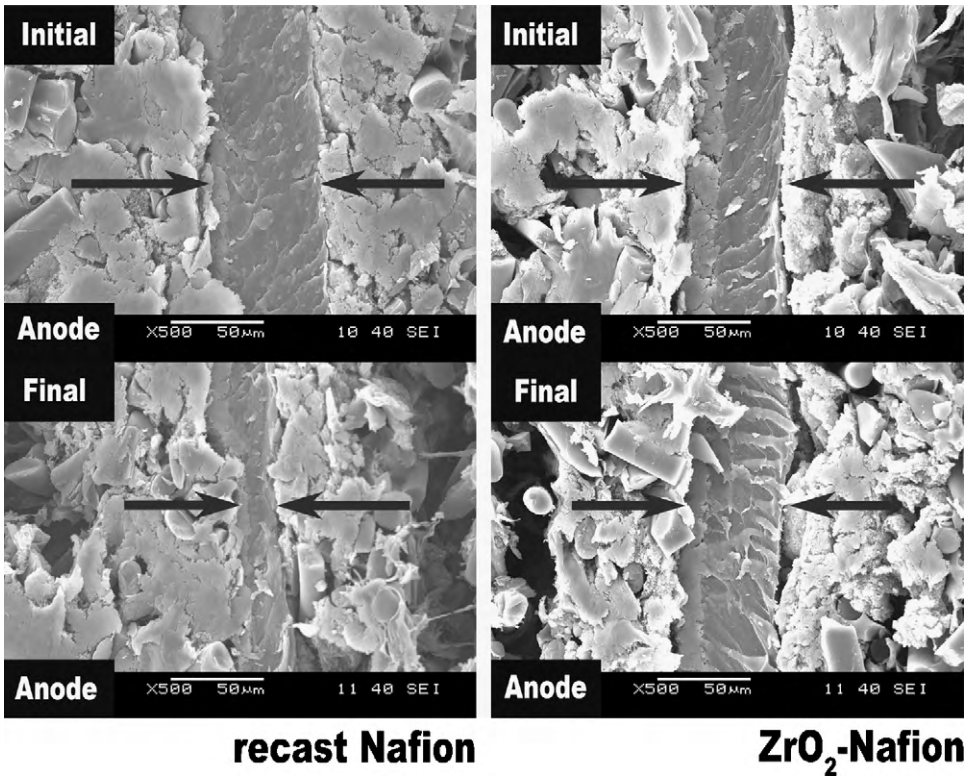

Fig. 7. Cross-section structures of different MEAs before and after OCV tests. The anode side is shown left here.

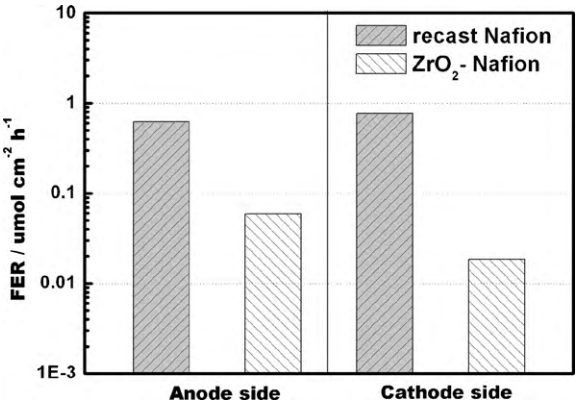

Fig. 8. FERs (μmol cm^{-2} h^{-1}) measured for recast Nafion and ZrO_2-Nafion MEAs during OCV test (cell temperature: 80 °C; saturator temperature: 64 °C; RH: 50%; anode gas: H_2; cathode gas: O_2; flow rate: 40 ml min^{-1} at anode and cathode; and duration: 24 h).

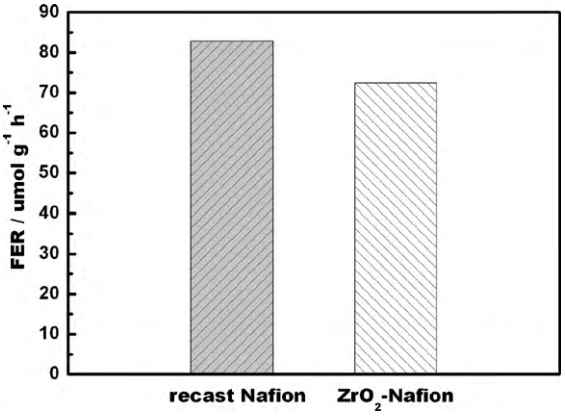

Fig. 9. FERs (μmol g^{-1} h^{-1}) measured for recast Nafion and ZrO_2-Nafion MEAs during Fenton test (Fenton solution: 30 wt.% H_2O_2 solution + 20 ppm Fe^{2+}; solution temperature: 80 °C; replacement of Fenton solution: 3 h; and duration: 30 h).

tures of MEAs before and after the OCV accelerated tests were determined by SEM (Fig. 7). In these images the left part is the anode catalyst layer, while the membrane is located in the middle. Thickness of the recast Nafion decreases dramatically relative to that of the initial membrane, suggesting that the chemical degradation takes place in the recast Nafion membrane during the OCV test. Higher gas permeation is subsequently obtained. By contrast, the cross-sectional morphology of the ZrO_2-Nafion membrane has no obvious change after 24 h OCV test, which can account for the stable limiting current of the ZrO_2-Nafion during the OCV test (Fig. 6).

FER is usually used to quantify the membrane degradation. As shown in Fig. 8, the incorporation of very small amount of ZrO_2 nanoparticles can almost reduce FER by up to one order of magnitude compared with the recast Nafion, and thereby produce a more durable membrane. The visible features include: (1) the lower OCV decay rate of the ZrO_2-Nafion than that of the recast Nafion in OCV test (Fig. 5); (2) the larger mount crossover hydrogen occurs in the recast Nafion based MEA (Fig. 6); (3) the discrepancy in the change rate of membrane thickness after the OCV test (Fig. 7).

3.4.2. *Ex situ accelerated Fenton test*

H_2O_2 has usually been considered to be the species indirectly (H_2O_2 decomposition to active oxygen radicals) responsible for the membrane degradation. The presence of the oxidizable metal ions such as Fe^{2+} is required to form the radicals from H_2O_2 [37]. Therefore, the Fenton test with Fe^{2+}, H_2O_2 solution and polymer mixed is employed to evaluate the membrane durability. In our Fenton test, hydrogen peroxide with high concentration (30 wt.% H_2O_2 solution and 20 ppm Fe^{2+}) was employed, and the Fenton solution was refreshed every 3 h to keep a relatively high H_2O_2 concentration in the solution [38]. The ZrO_2 nanoparticles embedded in membrane result in the decrease of FER (Fig. 9), which is in accordance with the conclusion drawn from Fig. 8.

Apart from the end group degradation pathway, chain scission pathways should be positive in the OCV accelerated test. Compared to the OCV test, the membrane degradation rate in the Fenton test is directly determined by the number of hydrogen-bearing end groups. FER rise by about one order of magnitude when unmitigated MEA are tested in the OCV test due to two different pathways, but FER in the Fenton test will rise very slowly because of the only end group degradation pathway [39]. The membrane mass loss during the Fenton test is 9.5% for the recast Nafion and 5.9% for the ZrO_2-Nafion, respectively.

3.5. *Electrochemical measurement*

In order to illustrate the reason why zirconia has the potential to mitigate the membrane degradation, Pt-ZrO_2/C was prepared and subjected to the RRDE measurement.

In the RRDE measurement, the percentage of H_2O_2 generated ($\chi_{H_2O_2}$) can be estimated from the following equation [14]:

$$\chi_{(H_2O_2)} = \frac{2I_R}{NI_D + I_R} \times 100$$

Where N (=0.37) is the collection efficiency in the RRDE measurement and I_R and I_D are the currents observed at the ring and the disk electrodes, respectively.

The results (Fig. 10) show the difference of H_2O_2 production between Pt/C and Pt-ZrO_2 (5 wt.%)/C. The amount of H_2O_2 reduces firstly and increases afterward with the decrease of the disk voltage. The impregnation of ZrO_2 distinctly reduces the production of H_2O_2, especially during the high voltage, suggesting that ZrO_2 has the potential to decompose hydrogen peroxide generated electrochemically on the Pt surface. The result means that the incorporation of ZrO_2 nanoparticles in the membrane can decompose hydrogen peroxide to water and oxygen. Hydrogen peroxide generated on the catalyst surface in the OCV test (where cathode

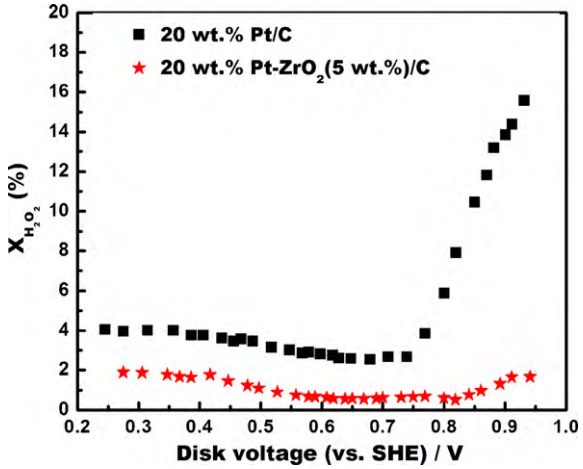

Fig. 10. RRDE results: percentage of H_2O_2 produced during oxygen reduction using Pt (20 wt.%)/C (baseline) and Pt (20 wt.%)-ZrO_2 (5 wt.%)/C hybrid electrocatalysts (temperature: room temperature; rotating rate: 1000 rpm; electrolyte used: 0.5 M H_2SO_4; ring potential was held constantly at 1 V vs. SCE, while disk potential was varied from 1 V vs. SCE to 0 V vs. SCE at a sweep rate of 10 mV s^{-1}).

potential is high, anode potential is low) or existed in the Fenton solution can diffuse into the membrane, and will be decomposed by the ZrO_2 embedded. By lowering hydrogen peroxide concentration in the membrane, the rate of generation of free-radicals can be also minimized.

4. Conclusions

A composite membrane using ZrO_2 nanoparticles as a hydrogen peroxide decomposition catalyst was firstly investigated in terms of the in situ OCV test and the ex situ Fenton test. ZrO_2 nanoparticles with size of 10 nm were prepared by the hydrothermal method and characterized by TEM and XRD. The incorporation of ZrO_2 nanoparticles in small quantities almost reduces FER by up to one order of magnitude relative to the recast Nafion, while the cell performance does not change significantly. Compared with the recast Nafion, the ZrO_2-Nafion based MEA exhibits an extremely stable OCV and no obvious thickness change of membrane. The OCV decay rates for the ZrO_2-Nafion and the recast Nafion are 0.8 mV h^{-1} and 6.6 mV h^{-1}, respectively. FERs of the Fenton test also indicate that ZrO_2 nanoparticles have the ability to improve the membrane durability. The ability of zirconia as a hydrogen peroxide catalyst is proven by the RRDE technique. It is proved that the incorporation of ZrO_2 nanoparticles is a promising approach to enhance the membrane durability.

Acknowledgements

We greatly acknowledge the financial support from the National Basic Research Program of China (973 Program No. 2010CB227202) and the National High Technology Research and Development Program of China (863 Program No. 2007AA05Z129).

References

[1] B. Smitha, S. Sridhar, A.A. Khan, J. Membr. Sci. 259 (2005) 10–26.
[2] S.M. Haile, D.A. Boysen, C.R.I. Chisholm, R.B. Merle, Nature 410 (2001) 910–913.
[3] S.D. Knights, K.M. Colbow, J. St-Pierre, D.P. Wilkinson, J. Power Sources 127 (2004) 127–134.
[4] A. Collier, H.J. Wang, X.Z. Yuan, J.J. Zhang, D.P. Wilkinson, Int. J. Hydrogen Energy 31 (2006) 1838–1854.
[5] F.D. Coms, H. Liu, J.E. Owejan, in: T. Fuller, K. Shinohara, V. Ramani, P. Shirvanian, H. Uchida, S. Cleghorn, M. Inaba, S. Mitsushima, P. Strasser, H. Nakagawa, H.A. Gasteiger, T. Zawodzinski, C. Lamy (Eds.), Proton Exchange Membrane Fuel Cells, vol. 8, 2008, pp. 1735–1747, Pts 1 and 2.
[6] S. Zhang, X. Yuan, H. Wang, W. Mida, H. Zhu, J. Shen, S. Wu, J. Zhang, Int. J. Hydrogen Energy 34 (2009) 388–404.
[7] W. Liu, D. Zuckerbrod, J. Electrochem. Soc. 152 (2005) A1165–A1170.
[8] N. Ramaswamy, N. Hakim, S. Mukerjee, Electrochim. Acta 53 (2008) 3279–3295.
[9] N. Ohguri, A.Y. Nosaka, Y. Nosaka, Electrochem. Solid State Lett. 12 (2009) B94–B96.
[10] P Trogadas, J. Parrondo, V. Ramani, Electrochem. Solid State Lett. 11 (2008) B113–B116.
[11] D. Zhao, B.L. Yi, H.M. Zhang, H.M. Yu, L. Wang, Y.W. Ma, D.M. Xing, J. Power Sources 190 (2009) 301–306.
[12] S. Babu, A. Velez, K. Wozniak, J. Szydlowska, S. Seal, Chem. Phys. Lett. 442 (2007) 405–408.
[13] P. Trogadas, V. Ramani, J. Power Sources 174 (2007) 159–163.
[14] N.R. de Tacconi, C.R. Chenthamarakshan, K. Rajeshwar, W.Y. Lin, T.F. Carlson, L. Nikiel, W.A. Wampler, S. Sambandam, V. Ramani, J. Electrochem. Soc. 155 (2008) B1102–B1109.
[15] T. Takane, H. Kato, H. Fujimoto, M. Ishikawa, Manufacture of Polymer Electrolyte Membrane for Fuel Cells, Involves Mixing Dispersion Liquid of Alkoxide of Element which Catalyzes Peroxide Decomposition, with Polyelectrolyte Solution, and Hydrolyzing and Condensing Alkoxide, Japan Gore Tex Inc., 2008.
[16] M. Ishikawa, H. Kato, T. Matsuura, T. Takane, Reinforced Solid Polymer Electrolyte Composite Film for Fuel Cell, has Polymer Electrolyte Membranes Provided at Both Surfaces, and Sheet-like Porous Reinforcing Material Containing Peroxide Decomposition Catalyst, Japan Gore Tex Inc., 2009.
[17] I. Gatto, A. Sacca, A. Carbone, R. Pedicini, E. Passalacqua, J. Fuel Cell Sci. Technol. 3 (2006) 361–365.
[18] B.P. Tripathi, V.K. Shahi, Colloid Surf. A 340 (2009) 10–19.
[19] C.M. Wang, E. Chalkova, C. Lute, M. Fedkin, S. Komarneni, T.C.M. Chung, S. Lvov, Proton Exchange Membr. Fuel Cells 8 (Pts 1 and 2) (2008) 1451–1459, 16.
[20] N.H. Jalani, R. Datta, J. Membr. Sci. 264 (2005) 167–175.
[21] A. Sacca, I. Gatto, A. Carbone, R. Pedicini, E. Passalacqua, J. Power Sources 163 (2006) 47–51.
[22] A. Sacca, A. Carbone, R. Pedicini, M. Marrony, R. Barrera, M. Elomaa, E. Passalacqua, Fuel Cells 8 (2008) 225–235.
[23] J.D. Kim, T. Mori, I. Honma, J. Electrochem. Soc. 153 (2006) A508–A514.
[24] Y. Zhang, H.M. Zhang, X.B. Zhu, C. Bi, J. Phys. Chem. B 111 (2007) 6391–6399.
[25] Y.Q. Song, C.L. Kang, Y.L. Feng, F. Liu, X.L. Zhou, J.A. Wang, L.Y. Xu, Catal. Today 148 (2009) 63–69.
[26] G. Liu, H.M. Zhang, Y.F. Zhai, Y. Zhang, D.Y. Xu, Z.G. Shao, Electrochem. Commun. 9 (2007) 135–141.
[27] X.Y. Geng, H.M. Zhang, Y.W. Ma, H.X. Zhong, J. Power Sources 195 (2010) 1583–1588.
[28] H.L. Tang, P.K. Shen, S.P. Jiang, W. Fang, P. Mu, J. Power Sources 170 (2007) 85–92.
[29] S. Kundu, L.C. Simon, M.W. Fowler, Polym. Degrad. Stab. 93 (2008) 214–224.
[30] M. Inaba, T. Kinumoto, M. Kiriake, R. Umebayashi, A. Tasaka, Z. Ogumi, Electrochim. Acta 51 (2006) 5746–5753.
[31] T. Kinumoto, M. Inaba, Y. Nakayama, K. Ogata, R. Umebayashi, A. Tasaka, Y. Iriyama, T. Abe, Z. Ogumi, J. Power Sources 158 (2006) 1222–1228.
[32] A. Kishi, M. Inoue, M. Umeda, J. Phys. Chem. C 114 (2010) 1110–1116.
[33] J.L. Bi, Y.Y. Hong, C.C. Lee, C.T. Yeh, C.B. Wang, International Symposium on Hydrogen from Renewable Sources and Refinery Applications, Atlanta, GA, 2006, pp. 322–329.
[34] G. Liu, H. Zhang, J.W. Hu, Electrochem. Commun. 9 (2007) 2643–2648.
[35] Y. Zhang, H.M. Zhang, Y.F. Zhai, X.B. Zhu, C. Bi, J. Power Sources 168 (2007) 323–329.
[36] C. Bi, H.M. Zhang, Y. Zhang, X.B. Zhu, Y.W. Ma, H. Dai, S.H. Xiao, J. Power Sources 184 (2008) 197–203.
[37] F.A. de Bruijn, V.A.T. Dam, G.J.M. Janssen, Fuel Cells 8 (2008) 3–22.
[38] F. Wang, H.L. Tang, M. Pan, D.X. Li, Int. J. Hydrogen Energy 33 (2008) 2283–2288.
[39] F.D. Coms, ECS Trans. 16 (2008) 235–255.